2013 IEEE/RSJ International Conference on
Intelligent Robots and Systems (IROS)
November 3-7, 2013. Tokyo, Japan

Design and Impedance Estimation of a Biologically Inspired Flexible Mechanical Transmission with Exponential Elastic Characteristic

Soumen Sen[1], *Member, IEEE*, Sananda Chatterjee[2], and Chandan Har[3]

***Abstract*— Nonlinear elasticity of transmission is indispensable in any passively variable stiffness mechanism. However, it remains obscure how to decide a desired nonlinear force-displacement function. On the other hand biological muscular actions are associated with stiffness/impedance variation in a wide range as demanded by everyday tasks. This paper addresses the issue of designing a nonlinear elastic transmission, where the elastic behaviour is obtained from the passive properties of biological muscle, which happens to be an *exponential* one, leading to existence of linearity between stiffness and force. In general, with passive damping, the transmission behaves as a mechanical impedance element, to be used in *variable impedance actuation*. Knowledge of the *varying* impedance is required to operate the transmission reliably. An off-line calibrated model can only be approximate and erroneous with noisy sensors and changing characteristics of the passive elements with time and environmental condition. This article implements an *Extended Kalman Filter* algorithm for on-line estimation of stiffness and impedance of such a damped series-elastic transmission. The underlined principle in *stiffness-force affine relation* is exploited favourably in stiffness estimation with reduced complexity. The effectiveness of the proposed estimator is examined through experiments on the mechanical transmission designed using the biological principle.**

I. INTRODUCTION

Introduction of flexibility and variation of intrinsic passive impedance is becoming essential in enhancing ability and performance of actuation systems in applications involving physical-human-robot-interaction including new generation of human friendly robots [1], exoskeletons and rehabilitation devices [2], prostheses and in legged locomotion [3]. In literature, Immega [4] by using pneumatic bladders, Goswami [5] with hydraulic cylinders, Mills [6] by employing a hybrid system of dc motor and pneumatic bladder have implemented variable stiffness mechanisms. Inherent unknown uncertainties, thermodynamic effects and packaging are some of the influencing drawbacks of these methods. On introducing stiffness variability in intrinsically safe flexible joint robots, Bicchi [1] achieved considerable performance enhancement, whereas Hurst [3] achieved efficient walking with nonlinear springs in legged locomotion. Essentially, all these approaches, (such as [1], [3], [7], [8], [9]), attempt to obtain stiffness variability through passive elastic elements with *nonlinear force-displacement* characteristics. However, the existing literature suggests little about how to make a choice of this nonlinear elastic function in general. On the other hand, the task of *simultaneous motion and stiffness* control can be achieved either explicitly, or antagonistically, or in combinations. The ubiquitous presence of agonist-antagonistic musculoskeletal actuation in the biological world sometimes motivates to go for an antagonistic implementation. Again, principles from the biology can be borrowed in search for a well grounded design principle of such a nonlinear elastic element. In this article, firstly, a principle is derived from experimentally validated behaviour of biological muscle fibre, from literature [10]. Then using the principle of virtual work, a general method for designing a mechanism (*cam* & *cam-profile*) is devised in order to exhibit the desired characteristic. The design of the nonlinear spring follows the work in [11], miniaturized for smaller deformation and higher load capacity and augmented with a damping element in parallel. Coincidentally, it carries similarity with the design in [12], but has been developed independently with a different principle and characteristic.

In simultaneous control of motion and impedance/stiffness, a difficult task remains in estimating the impedance components. An off-line static calibration and model based identification suffers from inaccuracies, un-modeled uncertainties, effect of sensor errors and drift in characteristics with time and environment condition. In order to avoid erroneous model based identification, Grioli [13] designed a *model-free* method in reconstructing time varying stiffness, using measurements of position and force and their time derivatives. The same authors in [14] proposed a dynamic stiffness observer, achieving ultimately bounded error stability. Serio [15] presented an EKF based stiffness observer, where, constant damping was assumed. Again, in a series of papers, Flacco [16], [17] avoided the use of extra force sensor in a novel way; however, not all the methods are proposed for real time implementation. These literatures also omit any report on sensor error modelling. In this article, a first order *Extended Kalman Filter* is proposed for estimation of stiffness with reduced complexity by making use of the *affine relation between stiffness and force*. For damping rate, a model is used, which follows the characteristic obtained from the manufacturer of the damper used. With force and position measurements and estimation of time rate of force, the EKF procedure estimates the impedance components. Sensor error models are also obtained experimentally.

II. PRINCIPLES FROM BIOLOGICAL MUSCLES

Nonlinearity in elasticity (and damping) is essential for passively variable stiffness (impedance) mechanism. Animal

[1,3] Robotics & Automation Div., CSIR-CMERI: Central Mechanical Engineering Research Institute, Govt. of India, Durgapur 713209, INDIA.
[2] Bengal Engineering and Science University & CSIR-CMERI Mechatronics Programme, INDIA
[1] Communicating author soumen.sen@ieee.org

978-1-4673-6357-0/13/$31.00 ©2013 IEEE

world in muscular actions carries out this variation quite effectively and efficiently and motivates to borrow a principle.

A. The Principle

Most of the models of biological muscle are still based on 1930s' A.V. Hill's model and subsequent contributions by A.F. Huxley. Two distinct behaviours of muscles are identified - one due to passive properties (without stimulations) and the other for the active properties. Muscles are found to become progressively stiffer on stretches. Pinto and Fung [10] observed experimentally (on rabbit heart muscle) that derivative of muscle *stress*, s with respect to *Lagrangian strain*, ε_L is proportional to stress at that point (left figure of Fig. 1). Therefore, $\frac{ds}{d\varepsilon_L} = \alpha(s+\beta)$, where $\varepsilon_L = \frac{L}{L_0}$, L_0 = rest length, L the current length and α and β are constants. Then, following is derived assuming constant cross section:

$$\frac{L_0}{A}\frac{dF_S}{dx} = \alpha\left(\frac{F_S}{A}+\beta\right), \tag{1}$$

where, $F_S \geq 0$ is the elastic force transmitted, A the constant cross sectional area and $x \geq 0$ is the elongation. Define, stiffness $\sigma = \frac{\partial F_S}{\partial x}$.

Proposition: Stiffness at a point of displacement being proportional to the force at that point leads to an *exponential* force-displacement characteristic,

$$F_S = \Phi(x) \; = \; \mu \, \exp\left(\frac{\alpha}{L_0}x\right) \; + \; F_0\,,\; x \geq 0\,, \tag{2}$$

where, α is an exponent and μ and $F_0 = -A\beta$ are constant coefficients.

Equation (2) is a solution of (1), which in normalized form can be expressed as

$$\sigma \; = \; \frac{\partial F_S}{\partial x} = \frac{\alpha}{L_0}\left(F_S + A\beta\right) \; = \; k_1 + k_2 F_S. \tag{3}$$

This relates stiffness and force *affinely*, (where, $k_2 = \frac{\alpha}{L_0}$ and $\frac{k_1}{k_2} = -F_0$). $\square$

B. Force Displacement Function from Spring Specification

Writing $F_S = \Phi(x)$, the relative force error is expressed as $\frac{\delta F_S}{F_S} = \frac{1}{\Phi(x)}\frac{d\Phi(x)}{dx}\delta x$. Let, the minimum sensible initial deflection of spring is δ_0 and corresponding relative force error is C_0. The relative force error of (2) at $x=0$ is computed as $\frac{\delta F_S}{F_S} = \frac{\alpha\mu\delta_0}{L_0(\mu+F_0)}$. At $x=0$, $F_0 = -\mu$ makes initial relative error undefined. For other values of F_0, there will be a force offset. An initial desired stiffness can be specified, which is equivalent to specifying initial force offset. Normally, the force offset is nonzero and the minimum controllable force is limited by dead band (backlash), dry friction and motor torque ripple.

For specified δ_0, relative force error at L_0 is given by,

$$C_0 \; = \; \frac{\mu \, \frac{\alpha}{L_0}\, \exp\left(\alpha\right)\, \delta_0}{\mu \, \exp\left(\alpha\right) + F_0}. \tag{4}$$

Defining dimensionless ratios, $F_{ratio} = \frac{F_{Smax}}{F_{Smin}}$, $L_{ratio} = \frac{X_{max}}{L_0}$, and $S_{ratio} = \frac{C_0 L_0}{\delta_0}$, the following nonlinear equation needs to be solved for α

$$\alpha \exp\left(\alpha\right)\left(F_{ratio}-1\right) + S_{ratio}\exp\left(\alpha\right) - S_{ratio}\exp\left(L_{ratio}\alpha\right) = 0, \tag{5}$$

For the chosen specification of maximum load capacity $F_{Smax} = 200$N, maximum deformation $X_{max} = 20$mm, $L_0 = 5$mm, minimum force $F_{Smin} = 5$N, $C_0 = 0.2$N/N and $\delta_0 = 1$mm, value of $\alpha = 1.3288$ is computed from (5) and following is obtained as a reasonable spring,

$$F_S = 0.9772\exp(0.2658x) + 1.2372,\; x \geq 0. \tag{6}$$

Fig. 1(right) shows both the designed and the calibrated spring force behaviour with deflection (see also Fig. 8(top)).

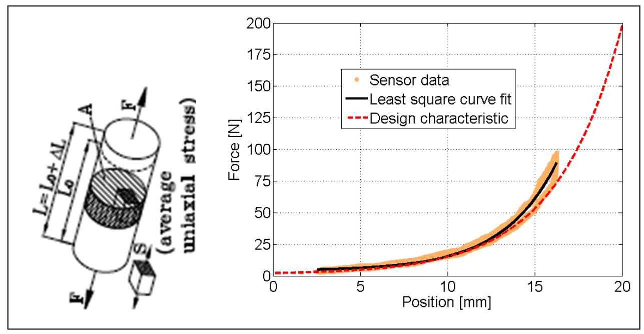

Fig. 1. (Left) Stress (s) developed across a muscle fibre under uniaxial tension according to [10]. (Right) The designed *force-displacement* characteristic, according to (6), is plotted in dashed line. Off-line least square curve fit is shown in solid line (see Table I). The deviation is due to lack of precise knowledge of stiffness of the linear spring on cam-follower, assumption of zero roller radius and inherent friction.

III. PHYSICAL REALIZATION OF NONLINEAR DAMPED ELASTIC TRANSMISSION

The physical realization of the spring follows the procedure described in [11], which attains the specified desired characteristic. Migliore et al. in [12] designed a spring with quadratic characteristic using cam profile. The present design is fundamentally different and has been developed independently. This approach applies *virtual work* principle, which is elegant, general and suitable for realizing any arbitrary continuous monotonic spring function (please refer to [11]).

A. Synthesis of Cam Profile

A spring loaded cam-follower on a cam profile is employed here. The desired characteristic in (2) is mapped on a Cartesian geometric plane using principle of virtual work (left figure of Fig. 2). Denoting $Y = \Psi(x)$ as the cam profile with Y being the displacement of the cam follower (loaded by a linear spring of fixed stiffness k_s) and $F_X = F_S$ be the elastic force along X, then application of principle of virtual work results into

$$\Psi(x) \; = \; \left(\frac{1}{k_s}\left\{\frac{\mu L_0}{\alpha}\exp\left(\frac{\alpha}{L_0}x\right) + F_0 x + C\right\}\right)^{\frac{1}{2}}, \tag{7}$$

where, C is constant of integration. Roller radius and rolling friction are neglected here. With initial condition of $\Psi(0) = 0$, $C = -\frac{\mu L_0}{\alpha}$.

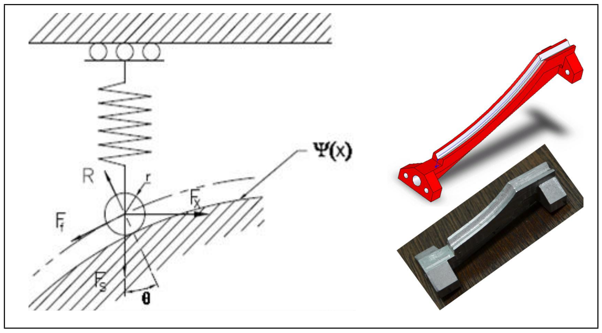

Fig. 2. (Left) Virtual work principle is applied to synthesize the geometric profile $\Psi(x)$. F_f is friction-force, R is the reaction, θ is the instantaneous contact angle, r be the roller radius. Linear spring is of stiffness k_s (see [11] for detail). (Right) CAD model of the designed exponential Cam profile and the actual machined component with Cam surface.

B. Manufacture of Cam Profile and Assembly of the Damped Elastic Transmission

The cam profile is realized in an aluminium block by CNC milling (Fig. 2). Two cam surfaces are used in opposition and the cam-followers are loaded by a linear spring with *design* spring constant of 5 N/mm; although the actual spring used in the spring assembly differs in the value of spring rate. A carriage containing the cam-followers is pulled by a rod; stiffness gets manifested at this rod end (see Fig. 3).

A nonlinear damping element is added in parallel with the elastic element by using an off-the-shelf *miniature damper* obtained from ACE GmBh, model FRT-D2-152. The force velocity characteristic from data sheet is well represented by an odd polynomial function

$$F_d = d_1\dot{x} + d_2\dot{x}^3, \tag{8}$$

where, d_1 and d_2, are constant coefficients. The damping element is shown in Fig. 3 and the identified damper characteristic at convergence is reported in Fig. 3(bottom) (also see Fig. 8 (bottom)).

The rotary damper and a miniature encoder of Hengstler make (model PC9S051204N) are mounted through a rotary-to-linear conversion. A miniature tensile force sensor of make Futek (model *FBB300*) is mounted at the pulling rod end to measure the transmission force. The assembly of the transmission is presented in the photograph of Fig. 3.

IV. IMPEDANCE OF A MECHANICAL TRANSMISSION

Impedance of a transmission is said to be the resistance experienced in changing the state (static/dynamic) of the transmission. Along with the elastic component a transmission can have a dissipation element, either inherently, or/and added on intentionally.

A. Nonlinear Transmission Model

The nonlinear transmission is modelled by a spring-damper-mass system,

$$F(t) = F_M(\ddot{x}(t)) + F_d(\dot{x}(t)) + F_\sigma(x(t)) + d_0\mathrm{sgn}(\dot{x}) + F_0\,,$$
$$\text{where, } F_M = m\ddot{x},\ F_S = F_\sigma + F_0, \text{ and } d_0 \text{ is the static friction.} \tag{9}$$

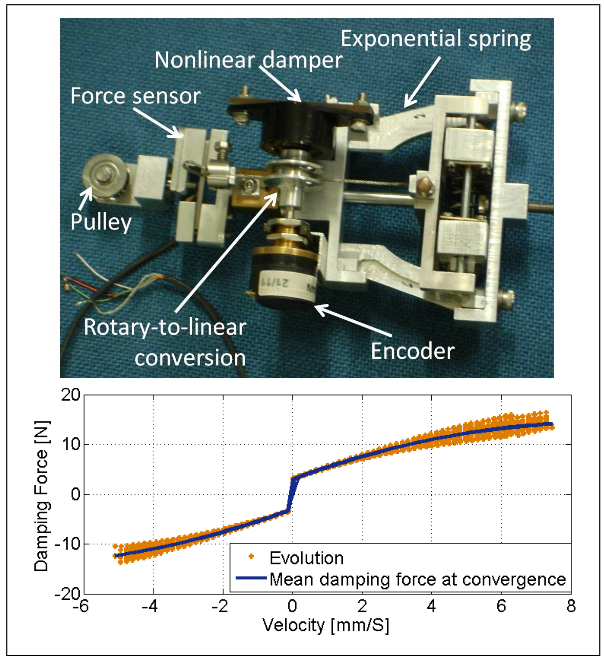

Fig. 3. (Top) The transmission assembly, showing the exponential spring and a nonlinear rotary damper in parallel through a rotary-to-linear conversion. An encoder is used to measure the displacement through the same mechanism. (Bottom) Damping characteristic obtained from a full model parameter estimation. d_2 is found to be negative. Static friction is identified; however, it is not needed in the impedance estimation in Sec. VI.

m is the inherent mass and F_S and F_d are given by (2) and (8) respectively. The implicit dynamic force balance in (9) can, therefore, be expressed as (in terms of unknown coefficients)

$$F = f(x, \dot{x}, \ddot{x}, d_0, d_1, d_2, \mu, k_2, F_0, m) \tag{10}$$

and the problem boils down to the task of identifying the unknown coefficients. To note that, k_2 does not appear linearly in (10), in contrary to other parameters. This problem is overcome in implementing the Extended Kalman Filter by estimating only the *stiffness*, exploiting the *affine relation* between stiffness and force (along with other impedance components).

B. Impedance of the Transmission

Given above, *impedance* components are defined as

$$\begin{array}{ll} \text{Generalized } \textit{Stiffness}: & \sigma = \frac{\partial f}{\partial x} \\ \text{Generalized } \textit{Damping} \text{ rate}: & D = \frac{\partial f}{\partial \dot{x}} \\ \text{Generalized } \textit{Inertia}: & M = \frac{\partial f}{\partial \ddot{x}} \end{array} \tag{11}$$

and the following differential form is obtained:

$$\delta F = M\delta\ddot{x} + D\delta\dot{x} + \sigma\delta x. \tag{12}$$

In practice, it is very difficult (especially in steady state) to directly measure the impedance components by evaluating the ratios of respective differential forces and differential motions. One direct method for estimating the impedance components (stiffness, damping-rate and inertia) requires precise knowledge of the elastic and damping models. Differently, here an attempt is made in estimating the generalized impedance components of (11) *not* using the direct force model of (10), but following a novel approach through exploiting the *affine stiffness-force relation*.

C. Exploiting the Affine Stiffness-Force Relation

The design principle chosen allows to take this approach, so that, only few of the unknown coefficients (here,only k_2) need to be estimated, which is appearing linearly. The following derivative is assumed to exist

$$\dot{F}(t) = \frac{\partial F_S}{\partial x}\dot{x}(t) + \frac{\partial F_d}{\partial \dot{x}}\ddot{x}(t) + \frac{\partial F_M}{\partial \ddot{x}}\dddot{x}(t), \tag{13}$$

such that $\dot{F} = \sigma\dot{x} + D\ddot{x} + M\dddot{x}$ using definitions in (11).

1) Case- constant damping: Time rate of stiffness is given by

$$\dot{\sigma}(t) = k_2\sigma\dot{x}, \text{ and } \dot{D} = 0, \ \dot{M} = 0. \tag{14}$$

A small constant damping is considered to be present in linear ball-bushes in the spring assembly. Equations (13) and (14) are used in the EKF formulation in estimating the states x, $\dot{x}$ and $\ddot{x}$ and the impedance components $\sigma(t)$, $D = d_1$ and $M = m$. The pretension force F_0 and the static friction d_0 can be estimated in a parallel filter (which may be slower) based on the total measured force and the total estimated impedance force. This formulation requires the time rate of change of force, which is obtained by using a filter on the force data.

2) Case- nonlinear damping force: From the damper characteristic in (8), time derivative of the damping rate is:

$$\dot{D} = 6d_2\dot{x}\ddot{x} \tag{15}$$

V. PARAMETER ESTIMATION: INITIALIZATION

The transmission here is designed to have some desired behaviour and a first order EKF is devised for impedance estimation. Like any other algorithm based on Kalman filter, the convergence of the procedure remains highly sensitive to the initial guess of the unknown states and parameters. To improve the convergence, an initialization procedure is proposed, based on a weighted least square method. In doing so, firstly, sensor error (noise) models are obtained experimentally, along with their variance.

A. Sensors and their Error Models

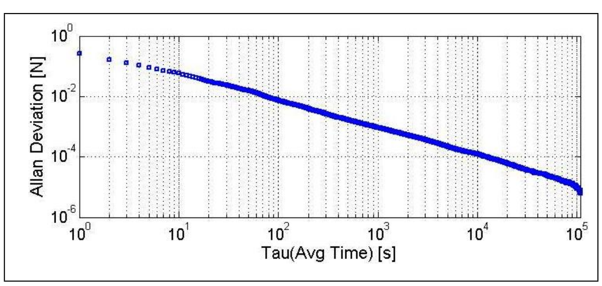

Fig. 4. Allan variance plot of force sensor data, indicating a constant slope of -1 approximately for white nature of the noise.

The experimental configuration is shown in Fig. 5. A pre-calibrated standard force gauge of IMADA make (model *DS2-200N*) is used as reference for determining the force sensor error model and calibration. Data are logged at 100 Hz frequency for a long time in a National Instruments based data acquisition system using Labview®. The *white* nature of the noise is more or less observed from nearly constant slope of *Allan Variance* plot in Fig. 4 (see [18]). Similarly, noise pattern of force-rate is found to be more or less white in nature, obtained in another experiment with a constant ramp input. The encoder error model is taken from [19], which has been carried out in CSIR-CMERI, India. Encoder noise as well is found to be *white* in nature. Variances of the sensors are obtained as 0.017N (force), 0.088N/s (force-rate) and 0.01mm (position) respectively.

TABLE I

INITIAL PARAMETER VALUES FROM OFFLINE ESTIMATION PROCEDURE.

Initial	d_0	d_1	d_2	μ	k_2	F_0	m
Mean	3.8221	1.8446	-0.0108	0.9251	0.2586	4.199	0.3959
Variance	0.1835	0.0193	0.0024	0.0012	–	0.1741	0.0401

B. Initialization - Identifying Initial Model Parameters

Except k_2, all the parameter coefficients of the elastic and damping function appear linearly in respective relationships. Therefore, initial k_2 is identified off-line using a *nonlinear least square fit*. Initial identification of all other unknown parameters are then refined by solving a over-constrained system of simultaneous equations in (16). Defining $X = \begin{bmatrix} m & d_0 & d_1 & d_2 & \mu & F_0 \end{bmatrix}^T \in \mathbb{R}^q$, $q = 6$,

$$\mathscr{F} = AX + \mathscr{W}, \tag{16}$$

where $\mathscr{F} \in \mathbb{R}^p$; $\mathscr{W} \in \mathbb{R}^p$ is a zero mean disturbance vector with $E[\mathscr{W}\mathscr{W}^T] = R_w$, $A \in \mathbb{R}^{p\times q}$ have entries from logged and estimated data of position, velocity, acceleration, p being the number of logged data set. A minimum variance least square estimate, $\hat{X}$ and its variance, R_X, can be obtained as (see [20]):

$$\hat{X} = (A^T R_w^{-1} A)^{-1} A^T R_w^{-1} \mathscr{F}, \tag{17}$$

$$R_X = E[(\hat{X} - X)(\hat{X} - X)^T] = (A^T R_w^{-1} A)^{-1}. \tag{18}$$

The obtained initial parameter values are indicated in Table I, having consistent units.

VI. IMPEDANCE AND STATE ESTIMATION BY AN EKF PROCEDURE

In this *EKF* framework for simultaneous state, parameters and impedance estimation, only k_2 and d_2 appear in the state vector, according to the derivation in section IV-C. It estimates generalized stiffness (σ), generalized damping rate (D) and generalized inertia (M), rather than the elastic and damping model parameters. The input to the estimator includes time rate of force, which is obtained using a filter from the force-sensor data. Measurement is the deflection; velocity and acceleration are estimated within the filter.

The state vector considered in the estimator for nonlinearly damped transmission (*Case 2*) is $Z = \{z_i \,|\, i = 1 \text{ to } 8\} = \begin{bmatrix} x & \dot{x} & \ddot{x} & \sigma & D & M & k_2 & d_2 \end{bmatrix}^T$.

The *input* to the state estimator is force-rate, whereas, *encoder* is used for observation. With sampling time T for the discrete system, the state equations are described below:

$$\begin{aligned}
z_1^{k+1} &= z_1^k + T z_2^k, \\
z_2^{k+1} &= z_2^k + T z_3^k, \\
z_3^{k+1} &= z_3^k - \frac{(z_2^k z_4^k + z_3^k z_5^k)T}{z_6^k} + \frac{\dot{F}(k)T}{z_6^k}, \\
z_4^{k+1} &= z_4^k + 3 z_2^k z_4^k z_7^k T, \\
z_5^{k+1} &= z_5^k + 18 z_2^k z_3^k z_8^k T, \\
z_6^{k+1} &= z_6^k, \quad z_7^{k+1} = z_7^k, \quad z_8^{k+1} = z_8^k.
\end{aligned} \tag{19}$$

VII. EXPERIMENTAL SETUP

The experimental setup is shown in Fig. 5. The transmission is pulled by a geared dc motor, configured as a position actuator, with a wire rope. One end of the transmission is hanged on the digital force-gauge and force-sensor is attached on the pulling rod at the motor side. Data are logged at a frequency of 100 Hz.

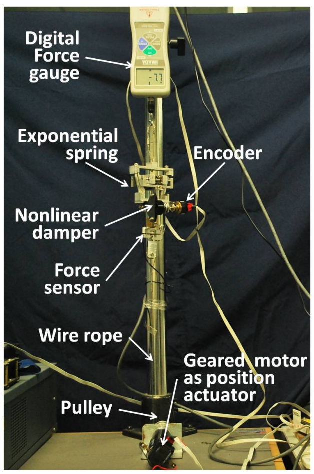

Fig. 5. Experimental setup. Locations of the sensors are shown.

VIII. RESULTS AND DISCUSSION

Good convergence is obtained in both the states and parameters/impedance estimation in experiments. Estimated values of the impedance components and the required model parameters at convergence are tabulated in Table II for the damped elastic transmission (*Case 2*). Input to the EKF estimator is force and its derivative, which is obtained passing through a first order filter and reported in Fig. 6. Estimated kinematic states are presented in Fig. 7. The identified stiffness characteristic with mean values at convergence and the mean characteristic of the damper are presented in Fig. 8. d_2 is found to be negative, confirming the nature of the damper obtained from the data sheet. The variances indicate good repeatability (Table II).

Linearly damped transmission (*Case 1*) is used solely to find the elastic characteristic. Here, only the results on the nonlinearly damped transmission (*Case 2*) are reported.

TABLE II

PARAMETER VALUES AND IMPEDANCE COMPONENTS AT CONVERGENCE

	d_2	k_2	σ	D	m
Mean	-0.1063	0.2601	Varying	Varying	0.055
Variance $\times 10^{-4}$	0.928	0.849	16.6	10.79	0.644

Generalized stiffness and damping rate are estimated at every time update step and it is seen that estimation converges reasonably well. Tracking estimation of the impedance components are reported in Fig. 9.

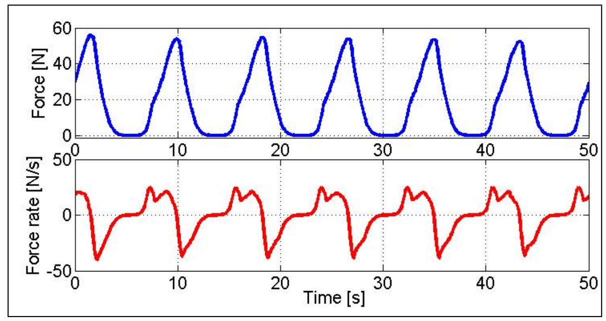

Fig. 6. (Top) Input force sensor reading. (Bottom) Estimated force rate.

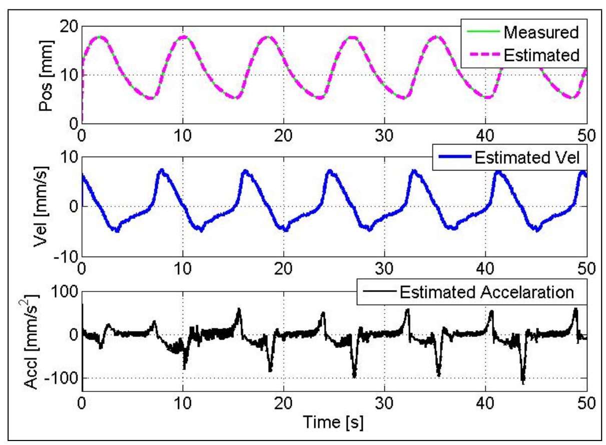

Fig. 7. (Top) Measured and estimated position, (Middle) estimated velocity, and (Bottom) estimated acceleration of deflection of the transmission. Actual values of velocity and acceleration are not measured.

IX. CONCLUSIONS

The article presents a novel design of a nonlinear elastic transmission (added with nonlinear damping), starting from a first principle derived from biological muscle property. The resulted characteristic happens to be an exponential one, which possesses the advantageous property of linearity between stiffness and elastic force of the transmission. Again, it has been reported in [11] that a spring with an *exponential* force-displacement function behaves fastest among a class of power springs in moving from one higher stiffness value to a lower value with same stored initial potential energy.

The article proposes an *Extended Kalman Filter* based procedure for on-line estimation of transmission impedance.

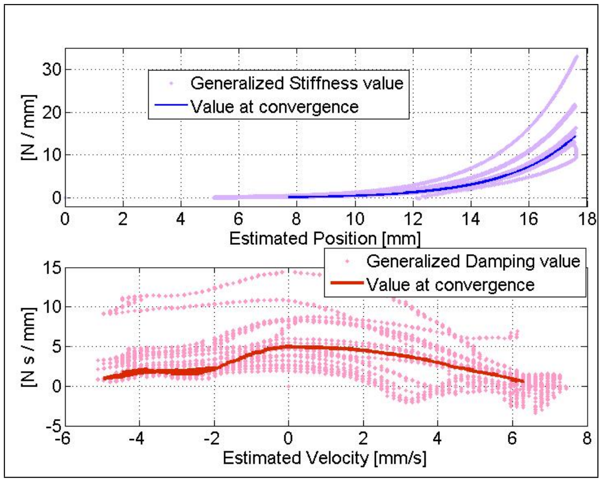

Fig. 8. (Top) Evolution of estimation of stiffness (mean values) plotted over the identified stiffness characteristic at convergence. (Bottom) Similar evolution of damping rate plotted over the identified values at convergence.

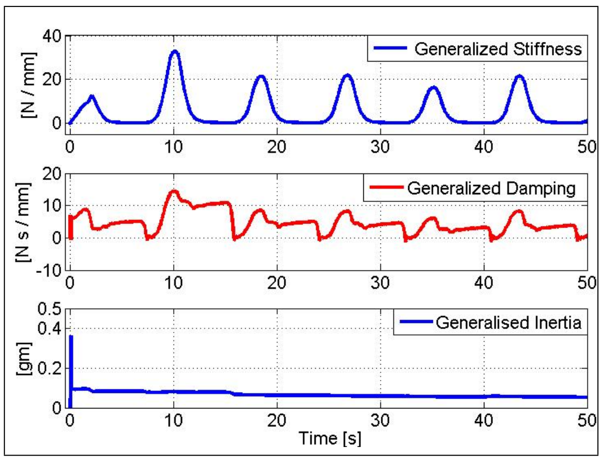

Fig. 9. Tracking of impedance components. (Top) Generalized *Stiffness*, (Middle) Generalized *Damping*, and (Bottom) Generalized *Inertia*.

In contrary to conventional methods for parameter estimation of transmission function, the proposed procedure exploits the *affine stiffness-force* relationship in estimating the varying transmission stiffness. In estimating the impedance components (stiffness, damping rate and inertia), not all model parameters appear in the EKF formulation and thereby reduces the complexity of the procedure. However, the convergence is sensitive on the choice of initial parameter states (reduced) and their covariance. It is proposed to obtain these initial values through an off-line identification procedure. A *weighted least square* method is employed with the *sensor covariance matrix* as the weighting matrix. It is claimed that good convergence can be obtained in this way. The implementation assumes an approximate model, which is justified - the design of the nonlinear transmission is not arbitrary; rather follows an optimal functional behaviour. Nevertheless, the method suffers from the inherent limitation of indeterminacy of accuracy (like any other EKF), but achieves good repeatability. Force rate is taken as input with an approximate variance obtained from limited experiments. It is kept as future work to obtain the error model of the force rate through extensive experiments.

X. ACKNOWLEDGMENTS

The work is done within the CSIR-CMERI institute project OLP152312. The first author also expresses his sincere gratitude to Prof. Antonio Bicchi, Interdepartmental Research Centre E. Piaggio, Univ. of Pisa, Italy for discussions.

REFERENCES

[1] A. Bicchi, and G. Tonietti, Fast and Soft Arm Tactics: Dealing with the Safety–Performance Tradeoff in Robot Arms Design and Control, IEEE Robotics and Automation Mag., vol.11, no.2, Special issue on “Safety Among Us”, June, 2004.

[2] M.S. Cherry, D.J. Choi, K.J. Deng, S. Kota, and D.P. Ferris, Design and fabrication of an elastic knee orthosis - preliminary results, in ASME IDETC/CIE, Philadelphia, 2006.

[3] J.W. Hurst, J.E. Chestnutt, and A.A. Rizzi, An actuator with physically variable stiffness for highly dynamic legged locomotion, in Proc. IEEE Int. Conf. on Robotics and Automation, New Orleans, 2004.

[4] G.B. Immega, Romac: Actuators for Micro Robots, in IEEE Micro Robotics and Teleoperators Workshop, Hyannis, Massachusetts, 1987.

[5] A. Goswami, M.A. Peshkin, and J.E. Colgate, Passive Robotics: An Exploration of Mechanical Computation, in Proc. IEEE Int. Conf. on Robotics and Automation, Cincinnati, May, 1990, pp.279-284.

[6] J.K. Mills, Hybrid Actuator for Robot Manipulators: Design, Control, and Performance, in Proc. IEEE Int. Conf. on Robotics and Automation, Cincinnati, May, 1990, pp.1872-1878.

[7] R. Schiavi, G. Grioli, Soumen Sen, and A. Bicchi, Vsa-II: a novel prototype of variable stiffness actuator for safe and performing robots interacting with human, in Proc. IEEE Int. Conf. on Robotics and Automation, Pasadena, 2008.

[8] S. Wolf, and G. Hirzinger, A new variable stiffness design: Matching requirements of the next robot generation, in Proc. IEEE Int. Conf. on Robotics and Automation, Pasadena, 2008.

[9] A. Jafari, N Tsagarakis, B. Vanderborght and D. Caldwell, A novel actuator with adjustable stiffness (AwAS), in Proc. IEEE/RSJ Int. Conf. on Intelligent Robots and Systems, pp. 4201-4206, 2010.

[10] J.G. Pinto, and Y.C. Fung, Mechanical Properties of the Heart Muscle in the Passive State, J. of Biomechanics, vol.6, 1973.

[11] Soumen Sen and Antonio Bicchi, A Nonlinear Elastic Transmission for Variable-Stiffness-Actuation: Objective and Design, in Proc. 15^{th} National Conf. on Machine and Mechanisms, Chennai, Nov.29-Dec.01, 2011.

[12] S.A. Migliore, E.A. Brown, and S.P. DeWeerth, Biologically inspired joint stiffness control, in Proc. IEEE Int. Conf. on Robotics and Automation, Barcelona, April, 2005.

[13] G. Grioli and A. Bicchi, A Non-Invasive, Real-Time Method for Measuring Variable Stiffness, in Proc. Robotics Science and Systems (RSS 2010), Zaragoza, E, June 2010.

[14] G. Grioli and A. Bicchi, A real-time parametric stiffness observer for VSA devices, in Proc. IEEE Int. Conf. on Robotics and Automation, Shanghai, May, 2011.

[15] A. Serio, G. Grioli, I. Sardellitti, N. G. Tsagarakis and A. Bicchi, A decoupled impedance observer for a variable stiffness robot, in Proc. IEEE Int. Conf. on Robotics and Automation, Shanghai, May 2011.

[16] F. Flacco and A. De Luca, Residual-based stiffness estimation in robots with flexible transmissions, in Proc. IEEE Int. Conf. on Robotics and Automation, Shanghai, May, 2011.

[17] F. Flacco, A. De Luca, I. Sardellitti and N. G Tsagarakis, On-line estimation of variable stiffness in flexible robot joints, in Int. J. of Robotic Research, 31(13), pp. 1556-1577, Oct. 2012.

[18] N. El-Sheimy, H. Hou, and X, Niu, Analysis and Modeling of Inertial Sensors Using Allan Variance, IEEE Tran. on Instrumentation and Measurement, Vol.57, No.1, Jan., 2008.

[19] S. Jain, S. Nandy, G. Chakraborty, C. S. Kumar, R. Ray and S. N. Shome, Error Modeling of various sensors for Robotics application using Allan Variance Technique, in Proc. IEEE Int. Conf. on Sig. Pro., Com., and Comp. (ICSPCC-2011), Xian, China, Sep. 2011.

[20] R. Plackett, Some theorems in least squares, Biometrika, 37 (1-2), pp. 149-157, 1950.